# Experimental observation of a Raman-induced temporal waveguide

Junchi Zhang [1], William Donaldson,[2] and Govind P. Agrawal [1,2]
[1]*The Institute of Optics, University of Rochester, Rochester, New York 14627, USA*
[2]*Laboratory of Laser Energetics, University of Rochester, Rochester, New York 14627, USA*

The formation of a Raman-induced temporal waveguide is demonstrated by launching short pump and probe pulses inside a photonic crystal fiber. The pump pulse creates a fundamental soliton whose speed changes continuously owing to its deceleration through the Raman-induced red shift of its spectrum. The spectrum of the probe pulse is blue-shifted to ensure that the two pulses move at the same speed and follow the same trajectory over the entire length of the fiber. The output wavelengths of the pump and probe pulses depend on the peak power of input pump pulses and their measured values agree with the predictions based on the dispersion data. Numerical modeling also shows good agreement with the experimental results.

## I. INTRODUCTION

Although propagation of electromagnetic waves in a time-varying medium was considered as early as 1958 [1], it is only over the last 20 years that this topic has been studied extensively [2–16]. Temporal variations in the electrical permittivity of a medium lead to a new degree of freedom that can be exploited for manipulating optical waves interacting with such a medium. For example, the reflection of light at a temporal boundary, with different refractive indices across it, induces a relatively large frequency shift [2,10]. Such frequency shifts occur because a temporal boundary breaks the time-translation symmetry. In another remarkable discovery, a photonic time crystal can be formed through periodic modulation of the refractive index in time [6,7]. Analogous to the energy band gaps forming in crystals with spatial periodicity, photonic time crystals exhibit a momentum gap, observed first in a 2004 experiment [16]. It was found that novel effects such as parametric amplification could occur in such momentum gaps [14,15].

A purely temporal modulation of the refractive index was considered in most previous studies. Under such conditions, modulation has to be fast on a timescale of the order of an optical cycle, and changes in the refractive index need to be large, of the order of unity. Such requirements have inhibited experimental observations of the predicted novel effects. When a traveling-wave-type modulation is applied to a dispersive medium, it was found that significant reflection of optical pulses can occur at a temporal boundary across which a much smaller index change occurs over a timescale shorter than the pulse's width, but much longer than a single optical cycle [5,9,10,17]. One can even realize the temporal analog of total internal reflection, with no field transmitted across the boundary. A moving temporal boundary can be created in an experiment by launching a short pump pulse into a nonlinear dispersive medium such as an optical fiber [17]. The refractive index increases, owing to the optical Kerr effect, only over the width of the pump pulse, resulting in the formation of a higher-index temporal window moving at the speed of the pump pulse.

One question worth asking is whether a temporal waveguide can be realized using such high-index regions. It was theoretically shown that a temporal waveguide can be formed using two boundaries that create a temporal window with a different refractive index than the surroundings and trap pulses between them [11,18]. In the context of supercontinuum generation, several studies showed that the trapping of a dispersive wave by a soliton can occur under certain conditions [19–27]. Interaction of a dispersive wave with a Raman soliton was also studied theoretically [28].

In this work we show that a single temporal boundary can also trap pulses through a cascaded temporal reflection process if its speed is not constant and changes in a continuous fashion. In practice, speed changes can occur through the Raman-induced frequency shift of short pump pulses propagating in an optical fiber [29]. In this work, we demonstrate the formation of such a temporal waveguide in a photonic crystal fiber (PCF) used as a nonlinear dispersive medium. By launching the pump and probe pulses at wavelengths on opposite sides of the PCF's zero-dispersion wavelength, we show that the probe pulse is forced to move at the speed of the pump pulse whose speed keeps decreasing because of a continuous red shift of its spectrum produced by the process of intrapulse Raman scattering [30]. A consequence of this speed matching is that the probe pulse undergoes a spectral blue shift all along the fiber, becoming as large as 70 nm at the end of the PCF in our experiment. As the amount of blue shift depends on the fiber's length and on the pump pulse's energy, this technique can be useful for tunable wavelength conversion of weak probe pulses, with potential applications in optical signal processing and quantum optics [31,32].

The paper is organized as follows. We use in Sec. II the underlying nonlinear Schrödinger's equation for studying numerically the temporal waveguiding process using parameters' values that correspond to our experiment. In Sec. III, we show our experimental setup and present the results acquired using a pump-probe configuration with varying delays between the two pulses. We discuss and summarize our main results in Sec. IV.

## II. NUMERICAL MODELING

We begin with numerical simulations of our experiment. When short optical pulses are injected in a single-mode fiber, their evolution is governed by a generalized nonlinear Schrödinger's equation of the form [30]

$$\frac{\partial A}{\partial z} + \sum_{k \geqslant 2} \frac{i^{k-1}}{k!} \beta_k \frac{\partial^k A}{\partial t^k} = i\gamma \left( 1 + \frac{i}{\omega_0} \frac{\partial}{\partial t} \right)$$
$$\times \left( A(z,t) \int_0^\infty R(t') |A(z, t - t')|^2 dt' \right), \quad (1)$$

where $A(z,t)$ is the pulse's envelope at a distance $z$, $\omega_0$ is the central frequency of the pulse, and $\beta_k$ is the $k$th-order dispersion parameter of the fiber. Here, $t$ is a reduced time measured in a moving frame and is related to the actual time $t_a$ as $t = t_a - z/v_g(\omega_0)$, where $v_g(\omega_0)$ is the group velocity at the frequency $\omega_0$. The nonlinear effects are included through the parameter $\gamma$ and the response function of the medium, $R(t) = (1 - f_R)\delta(t) + f_R h_R(t)$, where $h_R(t)$ is the Raman response and $f_R$ is its fractional contribution [30].

The optical Kerr effect is the most important nonlinear effect for short pulses launched into optical fibers. To understand its impact, we keep only the $k = 2$ term and choose $f_R = 0$ in Eq. (1). In this case, this equation takes the form of a Schrödinger equation with the potential $\gamma |A|^2$. It follows that pump pulses create an energy well or barrier depending on the nature of dispersion. When the wavelength of the probe pulses lies in the normal-dispersion region with $\beta_2 > 0$, the pump pulses create an energy barrier for probe pulses and reflect them partially. The frequency of the reflected part changes during reflection to ensure conservation of each photon's momentum [10].

For a probe pulse traveling faster than the pump pulse in the normal-dispersion region of the fiber, the reflected pulse travels slower than the pump pulse because its frequency shifts toward the blue side during the temporal reflection. In practice, it is useful to launch pump pulses at a wavelength for which $\beta_2 < 0$. In this situation, each pump pulse forms a soliton that creates a stable energy barrier whose shape does not change along the fiber. As the pump and probe pulses are in different dispersion regions, it is possible to choose their wavelengths such that they travel initially at nearly the same speeds.

Figure 1 shows the dispersion profile of the PCF used in our experiment (IXblue, IXF-SUP-2-135) by plotting measured values of its group index as a function of frequency. For these measurements, we use the technique based on white-light interferometry [33,34] with a supercontinuum laser (NKT Photonics). The two dots at the bottom show the initial central frequencies of the pump and probe pulses used in our experiments and in numerical simulations. Intrapulse Raman scattering is the second most important nonlinear effect for intense short pump pulses. The spectrum of a short pulse can be so wide that its high-frequency components amplify the low-frequency components of the same pulse through the Raman effect. The net result is that the central frequency of each pump pulse undergoes a continuous red shift as it propagates down the PCF. As a consequence of this red shift, the pump pulse decelerates when its spectrum lies in the
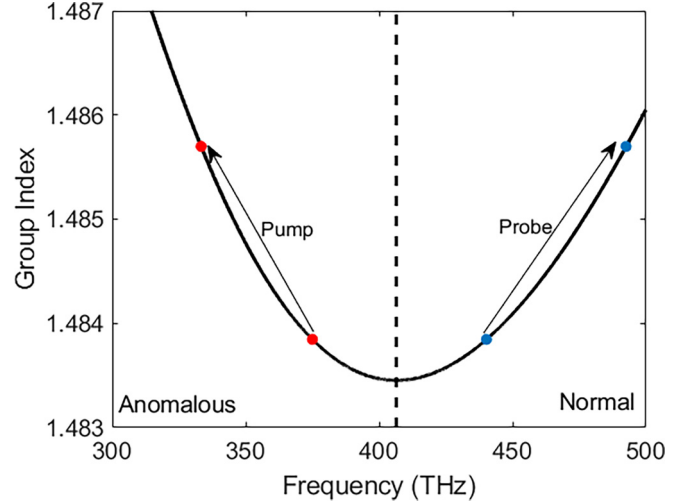


FIG. 1. Measured group index of our PCF plotted as a function of frequency. Dashed vertical line marks its zero-dispersion frequency (wavelength 738 nm). Two dots at the bottom mark the initial central frequencies of the pump and probe pulses. Two arrows show changes in these frequencies during their propagation inside the PCF.

anomalous region where $\beta_2 < 0$. As the pump pulse creates a moving high-index barrier for the probe pulse, this barrier also decelerates. When the pump-induced index change is large enough, the probe pulse is not able to tunnel through the barrier, and it must slow down to remain near the pump pulse. Slowing the probe pulse is possible only if its spectrum shifts toward the blue side.

Figure 2 shows the results of numerical simulations based on Eq. (1) with the parameters appropriate for our experiment. The pump pulse at 800 nm is launched into the 3.75-m-long PCF with its full width at half maximum (FWHM) about 110
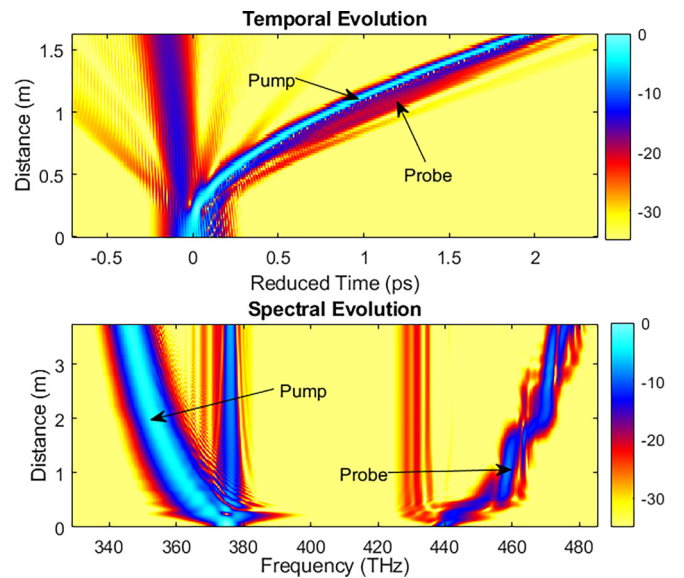


FIG. 2. Numerical simulations for a Raman-induced temporal waveguide. Probe pulse follows pump's trajectory because of its Raman-induced deceleration. Spectral evolution at bottom shows the red and blue shifts of the pump and probe pulses.

fs. It forms a a higher-order soliton (estimated soliton order 4.6). The probe pulse at 683 nm has a Gaussian shape with a FWHM of 137 fs (bandwidth 5 nm) and its group velocity is nearly matched to that of the pump pulse. The energy of the probe pulse was about 10% of the pump pulse. The low probe-pulse energy ensures that the probe has negligible impact on the pump. Dispersion parameters were obtained by fitting a polynomial to the measured dispersion data in Fig. 1.

As seen in Fig. 2, the higher-order soliton undergoes the process of soliton fission with in the first 20 cm of the PCF [30]. A short fundamental soliton is formed after the fission, which experiences intrapulse Raman scattering and its spectrum shifts toward the red side in a continuous manner all along the fiber. A red shift translates into a lower speed of the soliton, implying is continuous deceleration along the fiber. In the time domain, the soliton's trajectory follows a parabolic path because of this deceleration. The probe pulse follows this trajectory through temporal reflections that change its frequency in a zigzag fashion. The net result is that a Raman-induced temporal waveguide is formed that guides the probe pulse along the pump's trajectory. As the pump's spectrum red shifts, the spectrum of the probe pulse shifts toward the blue side because the two pulses experience opposite kinds of dispersion. The final frequencies of the pump and probe and the end of the PCF are shown by the two arrows in Fig. 1.

One can view the Raman-induced waveguiding process as a cascade of temporal reflections along the fiber's length. As the pump pulse slows down near the front end of the fiber, the probe reflects off the pump for the first time and blue shifts its frequency and becomes slower than the pump. However, after this first reflection, the pump pulse keeps slowing down and a second reflection occurs that shifts the probe's frequency further to the blue side. This process keeps repeating along the fiber's length. The net result is that a cascade of temporal reflections keeps the pump and probe pulses moving together along the entire length of the fiber. This interpretation is justified by the zigzag pattern of the blue shifts of the probe seen in Fig. 2, which is very different from the smooth spectral red shift of the pump. The total blue shift at the output end is such that the group velocities of the probe and pump pulses are nearly the same. In addition to the blue-shifted probe pulse, we still see some remaining unconverted probes. This is expected because a small portion of the probe can still tunnel through the pump pulse since it has a finite width.

## III. EXPERIMENT

In this section, we present and discuss our experimental results. Figure 3 shows the experimental setup schematically. A Ti:sapphire laser-pumped regenerative amplifier (Coherent, Astrella) emits a 1-kHz train of 100-fs pulses at 800 nm. Half of each pulse's energy pumps an optical parametric amplifier (OPA). The OPA generates white light from a small portion of the pump as seed and amplifies this seed through nonlinear wave mixing. Its output wavelengths are tunable over a wide range. A bandpass filter is used to reduce the spectral bandwidth to about 5 nm. We selected 683-nm probe pulses from the OPA and combined them using a beam splitter with the 800-nm pump pulses that were delayed suitably using a translation stage. The resulting beam is focused onto the
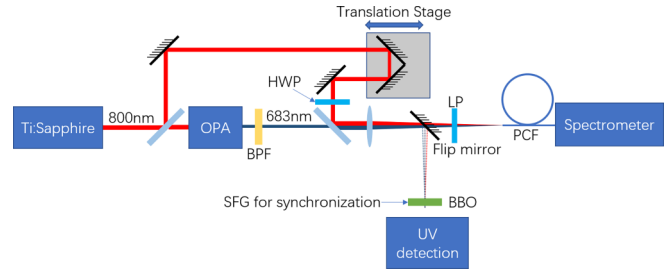


FIG. 3. Experimental setup. OPA: Optical parametric amplifier. BPF: bandpass filter. HWP: half-wave plate. LP: linear polarizer. PCF: photonic crystal fiber. SFG: sum frequency generation.

3.75-m-long PCF, and the spectrum of its output is measured with a spectrometer (Ocean Optics, USB2000+). A flip mirror sends the two beams to a BBO crystal for sum-frequency generation (SFG). The output is passed through a short-pass filter and sent into a spectrometer for UV detection. The SFG signal is used to synchronize the pump and probe pulses. The linear polarizer before the PCF ensures that the two pulses have the polarization direction that is aligned with one of the principal axes of the PCF. A half-wave plate is used in the pump beam's path to change the peak power of pump pulses.

Figure 4 shows the measured spectra from the PCF's output in three situations. When only the pump pulse with energy 9.7 pJ is launched, the spectrum in Fig. 4(a) contains two dominant peaks centered at 800 nm and 866 nm. The second peak corresponds to a fundamental soliton, formed after the fission of the pump pulse at a short distance into the PCF. Intrapulse Raman scattering has the most impact on this soliton, and its
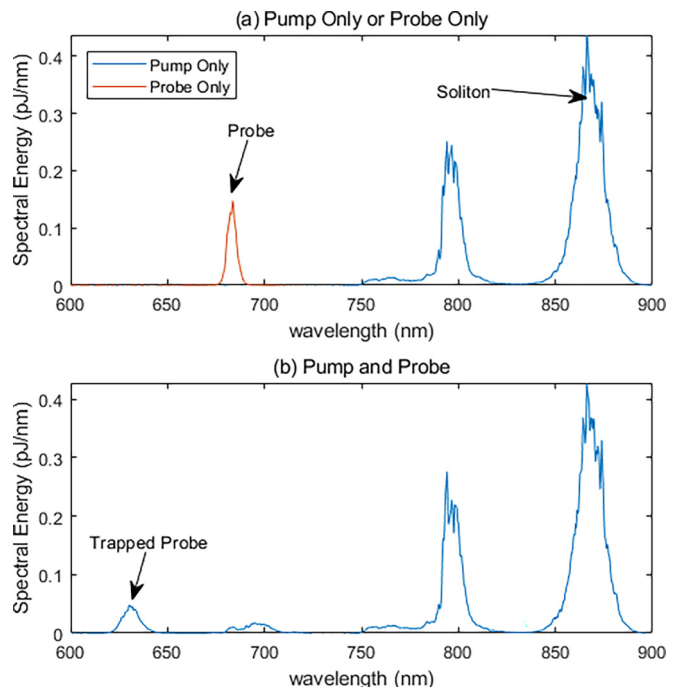


FIG. 4. Measured output spectra under different conditions. (a) Only the pump or probe pulse is sent through the PCF. (b) Both pump and probe pulses are sent through the PCF. Data are averaged over 25 000 pulses.
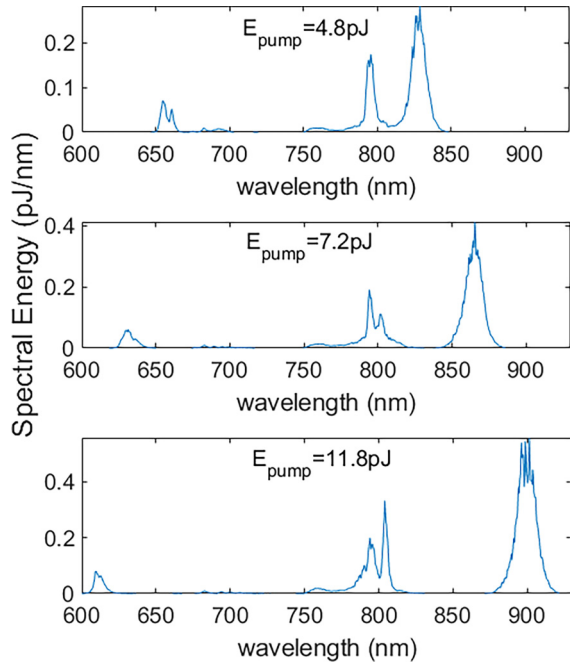
FIG. 5. Measured output spectra for three values of average pump pulse energy. Data are averaged over 2500 pulses.
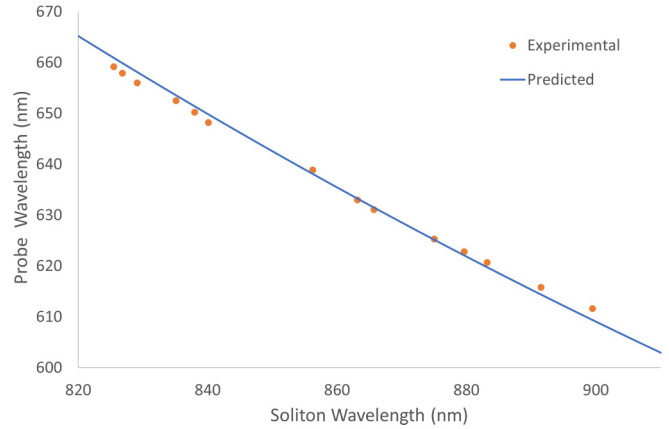


FIG. 6. Probe's output wavelength plotted as a function of soliton's wavelength (circles). Solid line is the prediction based on the dispersion data in Fig. 1.

spectrum red shifts all along the PCF. The remaining energy of the pump pulse appears as a peak around 800 nm. When only probe pulses are launched at 683 nm, a single peak at this wavelength is observed.

When both the pump and probe pulses are launched together into the PCF, as seen in Fig. 4(b), the output spectrum has a new blue-shifted peak at 631 nm. As expected, two peaks on the right side, formed through fission of the pump pulse, are not affected much by the probe pulse. In contrast, considerable energy of the probe pulse is blue shifted to near 631 nm. It can be seen from Fig. 1 that the group velocity at this wavelength matches with that of the red-shifted soliton at 866 nm. This matching indicates that a Raman-induced temporal waveguide is indeed formed inside our PCF.

The final wavelength of the probe pulse at the PCF's output depends on the peak power of the soliton formed after the fission of pump pulses. We verified this feature by varying the average pump power launched into the PCF. Figure 5 shows the measured spectra at three power levels. As we increase the pump power, the soliton's red shift becomes larger. As a result, the blue shift of probe pulses also becomes larger because of their Raman-induced temporal waveguiding.

The magnitude of the blue shift is set by the condition that the pump and probe pulses travel at the same speed inside the PCF. To verify this feature, we plot in Fig. 6 the measured blue-shifted wavelength as a function of the output wavelength of the soliton (circles). The soliton's wavelength is determined by fitting the spectrum to that of a "sech" pulse, while the probe's wavelength is based on the center-of-mass estimate. The solid line is obtained from the dispersion data shown in Fig. 1. It is evident that the probe's blue-shifted wavelength agrees quite well with the prediction based on group-velocity matching. The excellent agreement seen in

Fig. 6 is an indirect proof that a Raman-induced temporal waveguide did indeed form in our experiments.

A blue shift of the probe pulses induced by a decelerating pump pulse was also seen in Ref. [20]. In this work, a much longer dispersion-shifted fiber was employed, and the wavelengths of the pump and probe pulses was found in the infrared region on the opposite sides of the zero-dispersion wavelength near 1550 nm. The results were interpreted as trapping of the probe pulse by a soliton. Our work shows that this type of trapping is due to multiple reflections of a probe pulse from a curved temporal boundary created by the decelerating pump pulse. The probe pulse follows the path taken by the pump pulse by shifting its frequency to the blue side such that the two pulses move at nearly the same speed.

## IV. CONCLUSION

In this work, the formation of a Raman-induced temporal waveguide is demonstrated by launching short pump and probe pulses inside a photonic crystal fiber at wavelengths that lie on the opposite sides of the zero-dispersion wavelength of the fiber. Under such conditions, the pump pulse creates a fundamental soliton whose speed changes continuously owing to its deceleration through the Raman-induced red shift of its spectrum. We show that the spectrum of the probe pulse is blue shifted in a zigzag fashion along the fiber to ensure that the two pulses keep moving at nearly the same speeds over the entire length of the fiber. The output wavelengths of the pump and probe pulses depend on the peak power of input pump pulses and their measured values agree with the predictions based on the measured dispersion data. Numerical modeling also shows good agreement with the experimental results.

We explain the Raman-induced waveguiding process as a cascade of temporal reflections along the fiber's length that keeps the pump and probe probe pulses moving together along the entire length of the fiber. This interpretation is justified by the zigzag pattern of the blue shifts of the probe seen in Fig. 2. The blue shift of the probe pulses may be useful for tuning the wavelength of low-energy optical pulses toward the blue side using a suitable pump laser. Although four-wave mixing can also be used for this purpose, its use requires phase

matching. In contrast, our scheme makes use of intrapulse Raman scattering of pump pulses that does not require phase matching. It is the formation of a temporal waveguide that transfers the pump's Raman-induced red shift to the probe pulses as a blue shift. Our experiment shows that this shift can approach 100 nm in the visible region.

## ACKNOWLEDGMENTS

[1] F. R. Morgenthaler, Velocity modulation of electromagnetic waves, IEEE Trans. Microwave Theory Techn. **6**, 167 (1958).

[2] J. Mendonça and P. Shukla, Time refraction and time reflection: Two basic concepts, Phys. Scr. **65**, 160 (2002).

[3] F. Biancalana, A. Amann, A. V. Uskov, and E. P. O'Reilly, Dynamics of light propagation in spatiotemporal dielectric structures, Phys. Rev. E **75**, 046607 (2007).

[4] F. Biancalana, A. Amann, and E. P. O'Reilly, Gap solitons in spatiotemporal photonic crystals, Phys. Rev. A **77**, 011801(R) (2008).

[5] T. G. Philbin, C. Kuklewicz, S. Robertson, S. Hill, F. Konig, and U. Leonhardt, Fiber-optical analog of the event horizon, Science **319**, 1367 (2008).

[6] J. R. Zurita-Sánchez, P. Halevi, and J. C. Cervantes-Gonzalez, Reflection and transmission of a wave incident on a slab with a time-periodic dielectric function $\epsilon$ (t), Phys. Rev. A **79**, 053821 (2009).

[7] J. R. Zurita-Sánchez, J. Abundis-Patiño, and P. Halevi, Pulse propagation through a slab with time-periodic dielectric function $\epsilon$ (t), Opt. Express **20**, 5586 (2012).

[8] Y. Xiao, D. N. Maywar, and G. P. Agrawal, Reflection and transmission of electromagnetic waves at a temporal boundary, Opt. Lett. **39**, 574 (2014).

[9] K. E. Webb, M. Erkintalo, Y. Xu, N. G. Broderick, J. M. Dudley, G. Genty, and S. G. Murdoch, Nonlinear optics of fibre event horizons, Nat. Commun. **5**, 4969 (2014).

[10] B. W. Plansinis, W. R. Donaldson, and G. P. Agrawal, What is the Temporal Analog of Reflection and Refraction of Optical Beams? Phys. Rev. Lett. **115**, 183901 (2015).

[11] B. W. Plansinis, W. R. Donaldson, and G. P. Agrawal, Temporal waveguides for optical pulses, J. Opt. Soc. Am. B **33**, 1112 (2016).

[12] E. Lustig, Y. Sharabi, and M. Segev, Topological aspects of photonic time crystals, Optica **5**, 1390 (2018).

[13] K. Tan, H. Lu, and W. Zuo, Energy conservation at an optical temporal boundary, Opt. Lett. **45**, 6366 (2020).

[14] T. T. Koutserimpas, Parametric amplification interactions in time-periodic media: coupled waves theory, J. Opt. Soc. Am. B **39**, 481 (2022).

[15] Y. Sharabi, A. Dikopoltsev, E. Lustig, Y. Lumer, and M. Segev, Spatiotemporal photonic crystals, Optica **9**, 585 (2022).

[16] G. Van Simaeys, S. Coen, M. Haelterman, and S. Trillo, Observation of Resonance Soliton Trapping due to a Photoinduced Gap in Wave Number, Phys. Rev. Lett. **92**, 223902 (2004).

[17] L. Tartara, Frequency shifting of femtosecond pulses by reflection at solitons, IEEE J. Quantum Electron. **48**, 1439 (2012).

[18] B. W. Plansinis, W. R. Donaldson, and G. P. Agrawal, Cross-phase-modulation-induced temporal reflection and waveguiding of optical pulses, J. Opt. Soc. Am. B **35**, 436 (2018).

[19] N. Nishizawa and T. Goto, Characteristics of pulse trapping by use of ultrashort soliton pulses in optical fibers across the zero-dispersion wavelength, Opt. Express **10**, 1151 (2002).

[20] N. Nishizawa and T. Goto, Pulse trapping by ultrashort soliton pulses in optical fibers across zero-dispersion wavelength, Opt. Lett. **27**, 152 (2002).

[21] A. C. Judge, O. Bang, and C. M. de Sterke, Theory of dispersive wave frequency shift via trapping by a soliton in an axially nonuniform optical fiber, J. Opt. Soc. Am. B **27**, 2195 (2010).

[22] J. Travers and J. Taylor, Soliton trapping of dispersive waves in tapered optical fibers, Opt. Lett. **34**, 115 (2009).

[23] S. Hill, C. Kuklewicz, U. Leonhardt, and F. König, Evolution of light trapped by a soliton in a microstructured fiber, Opt. Express **17**, 13588 (2009).

[24] W. Wang, H. Yang, P. Tang, C. Zhao, and J. Gao, Soliton trapping of dispersive waves in photonic crystal fiber with two zero dispersive wavelengths, Opt. Express **21**, 11215 (2013).

[25] D. R. Austin, C. M. de Sterke, B. J. Eggleton, and T. G. Brown, Dispersive wave blue-shift in supercontinuum generation, Opt. Express **14**, 11997 (2006).

[26] D. V. Skryabin and A. V. Gorbach, Colloquium: Looking at a soliton through the prism of optical supercontinuum, Rev. Mod. Phys. **82**, 1287 (2010).

[27] R. Driben, F. Mitschke, and N. Zhavoronkov, Cascaded interactions between raman induced solitons and dispersive waves in photonic crystal fibers at the advanced stage of supercontinuum generation, Opt. Express **18**, 25993 (2010).

[28] S. Robertson and U. Leonhardt, Frequency shifting at fiber-optical event horizons: The effect of raman deceleration, Phys. Rev. A **81**, 063835 (2010).

[29] A. V. Gorbach and D. V. Skryabin, Light trapping in gravity-like potentials and expansion of supercontinuum spectra in photonic-crystal fibres, Nat. Photonics **1**, 653 (2007).

[30] G. P. Agrawal, *Nonlinear Fiber Optics*, 6th ed., (Academic, New York, 2019).

[31] D. Zhu, C. Chen, M. Yu, L. Shao, Y. Hu, C. Xin, M. Yeh, S. Ghosh, L. He, C. Reimer *et al.*, Spectral control of nonclassical light pulses using an integrated thin-film lithium niobate modulator, Light Sci. Appl. **11**, 327 (2022).

[32] L. J. Wright, M. Karpiński, C. Söller, and B. J. Smith, Spectral Shearing of Quantum Light Pulses by Electro-Optic Phase Modulation, Phys. Rev. Lett. **118**, 023601 (2017).

[33] P. Hlubina, M. Szpulak, D. Ciprian, T. Martynkien, and W. Urbańczyk, Measurement of the group dispersion of the fundamental mode of holey fiber by white-light spectral interferometry, Opt. Express **15**, 11073 (2007).

[34] T. Kardaś and C. Radzewicz, Broadband near-infrared fibers dispersion measurement using white-light spectral interferometry, Opt. Commun. **282**, 4361 (2009).